First Direct Mass Measurement of the Two-Neutron Halo Nucleus ^{6}He and Improved Mass for the Four-Neutron Halo ^{8}He

M. Brodeur,[1,2,*,†] T. Brunner,[1,3] C. Champagne,[1,4] S. Ettenauer,[1,2] M. J. Smith,[1,2] A. Lapierre,[1,†] R. Ringle,[1,†] V. L. Ryjkov,[1] S. Bacca,[1] P. Delheij,[1] G. W. F. Drake,[5] D. Lunney,[6] A. Schwenk,[7,8] and J. Dilling[1,2]

[1]*TRIUMF, 4004 Wesbrook Mall, Vancouver BC, Canada V6T 2A3*
[2]*Department of Physics and Astronomy, University of British Columbia, Vancouver, BC, Canada V6T 1Z1*
[3]*Physik Department E12, Technische Universität München, James Franck Straße, Garching, Germany*
[4]*Department of Physics, McGill University, Montréal, Québec, Canada H3A 2T8*
[5]*University of Windsor, Windsor ON, Canada*
[6]*CSNSM-IN2P3-CNRS, Université Paris 11, 91405 Orsay, France*
[7]*ExtreMe Matter Institute EMMI, GSI Helmholtzzentrum für Schwerionenforschung GmbH, 64291 Darmstadt, Germany*
[8]*Institut für Kernphysik, Technische Universität Darmstadt, 64289 Darmstadt, Germany*

(Received 8 July 2011; revised manuscript received 4 November 2011; published 31 January 2012)

The first direct mass measurement of ^{6}He has been performed with the TITAN Penning trap mass spectrometer at the ISAC facility. In addition, the mass of ^{8}He was determined with improved precision over our previous measurement. The obtained masses are $m(^6\mathrm{He}) = 6.018\,885\,883(57)$ u and $m(^8\mathrm{He}) = 8.033\,934\,44(11)$ u. The ^{6}He value shows a deviation from the literature of 4σ. With these new mass values and the previously measured atomic isotope shifts we obtain charge radii of 2.060(8) and 1.959 (16) fm for ^{6}He and ^{8}He, respectively. We present a detailed comparison to nuclear theory for ^{6}He, including new hyperspherical harmonics results. A correlation plot of the point-proton radius with the two-neutron separation energy demonstrates clearly the importance of three-nucleon forces.

DOI: 10.1103/PhysRevLett.108.052504 PACS numbers: 21.10.Dr, 21.10.Gv, 21.60.−n, 31.30.Gs

Nuclei with exceptionally weak binding lie at the limits of stability and exhibit fascinating phenomena. One of them is the formation of a halo structure of one or more loosely bound nucleons surrounding a tightly bound core, similar to electrons in atoms. The experimentally best studied cases are the two-neutron halo nuclei ^{6}He and ^{11}Li [1]. These nuclei are of Borromean nature, where all two-body (two-neutron and neutron-core) subsystems are unbound, but the three-body system is loosely bound [2]. Because of a lack of pairing correlations, the neighboring isotopes of ^{6}He (^{5}He and ^{7}He) are unbound, while ^{8}He is again bound with a four-neutron halo. This heaviest helium isotope also marks the nucleus with the most extreme neutron-to-proton ratio ($N/Z = 3$). Neutron halo nuclei are distinguished by their extended matter radius and a small neutron separation energy compared to other nuclei. The size of their core can be associated with the (root-mean-square) charge radius (its deviation from the halo-free core results from polarization effects due to strong interactions), while the halo extension depends exponentially on the separation energy [3].

To date, charge radii of halo nuclei can be determined only from the measurement of the change in energy of an atomic transition between isotopes A and A'. This so-called isotopic shift $\delta\nu^{A,A'}$ is linked to the mean-square charge radius difference $(r_c^2)^A - (r_c^2)^{A'}$ by

$$\delta\nu^{A,A'} = \delta\nu_{\mathrm{MS}}^{A,A'} + K_{\mathrm{FS}}[(r_c^2)^A - (r_c^2)^{A'}], \quad (1)$$

where the mass shift $\delta\nu_{\mathrm{MS}}^{A,A'}$ and the field shift constant K_{FS} are obtained using atomic structure calculations [4]. Because of their larger fractional change in mass and their smaller volume, light nuclei have a mass shift term typically $>10^4$ times larger than the field shift $\delta\nu_{\mathrm{FS}}^{A,A'} = K_{\mathrm{FS}}[(r_c^2)^A - (r_c^2)^{A'}]$. Furthermore, the mass shift sensitivity on the nuclear mass is such that reliable atomic masses with relative uncertainty on the order of 10^{-7} are needed in order for the mass uncertainty to make a negligible contribution to the charge radius determination of halo nuclei [5].

The nuclear charge radii of ^{6,8}He have been measured by laser spectroscopy [6,7]. However, to date, the mass of ^{6}He [8] is determined only from the Q-value comparison of two nuclear reactions [9] and has never been measured directly. Over the past years, direct Penning trap mass measurements have uncovered large deviations with indirectly measured masses, while yielding consistent results with other direct mass measurement methods (e.g., the 5σ deviation of the ^{11}Li mass [10]). Hence, a precise and accurate mass measurement of ^{6}He is highly desirable to update the charge radius analysis.

Understanding and predicting the properties of halo nuclei also presents a theoretical challenge. ^{6}He and ^{8}He are the lightest known halo nuclei and, due to their few-nucleon ($A \lesssim 10$) structure, are amenable to different *ab initio* calculations based on microscopic nuclear forces [11–15]. Therefore, they represent an ideal testing ground for nuclear structure theory, leading to a deeper understanding of the strong interaction in neutron-rich systems.

In this Letter, we present the first direct mass measurement of ^{6}He, together with a more precise value for ^{8}He, using the TRIUMF Ion Trap for Atomic and Nuclear science (TITAN) [16] Penning trap mass spectrometer. The TITAN facility is situated in the low-energy section of TRIUMF's Isotope Separator and ACcelerator (ISAC) experimental hall [17]. The ^{8}He mass was first directly measured in an earlier TITAN experiment [18]. Based on the new masses presented here, we determine reliable binding energies and the resulting values for the charge radii r_c of ^{6}He and ^{8}He. These observables provide key tests for nuclear theory. We make a detailed comparison to theory for ^{6}He, where *ab initio* calculations based on different nucleon-nucleon (NN) and three-nucleon ($3N$) forces are available. To date, no calculation exists based on chiral effective field theory interactions. This approach has the advantage that the corresponding $3N$ and $4N$ forces are largely predicted. As a first step towards this goal, we present new *ab initio* hyperspherical harmonics results based on chiral low-momentum interactions. A natural correlation between separation energy and radii is found when only NN interactions are included. The results and the precise experimental data clearly illustrate the importance of including $3N$ forces.

Both radioactive helium isotopes were produced via spallation reaction using 500 MeV protons from the TRIUMF cyclotron at a current of 80 μA impinging a high power silicon-carbide target. The beam was ionized using the forced electron beam ion arc discharge source [19] and transported at an energy of 20 keV to the TITAN facility. Contamination in both beams was removed using a two-stage high resolving power dipole-magnet mass separator. Upon reaching the TITAN facility, the purified continuous ion beam was thermalized, accumulated, and bunched using a hydrogen-filled radio frequency quadrupolar (RFQ) ion trap [20]. After their extraction from the RFQ, the ions were transported at an energy of approximately 1 keV to the Penning trap, where the mass measurement was performed.

The basic principle behind Penning trap mass spectrometry consists of measuring the cyclotron frequency $\nu_c = qB/(2\pi M)$ of an ion of mass M and charge q in a magnetic field B. TITAN, like most on-line Penning trap mass spectrometers, uses the time-of-flight ion-cyclotron resonance (TOF-ICR) technique [21,22] to determine the ion's cyclotron frequency (we refer the reader to [23,24] for more details about mass measurements using the TOF-ICR technique at TITAN).

Typical ^{6}He$^+$ and ^{8}He$^+$ time-of-flight ion-cyclotron resonances are shown in Fig. 1. These measurements took 27 min each and comprised 1656 and 1171 detected ions yielding statistical relative uncertainties on the cyclotron frequencies of 9 and 14 ppb, respectively. For both isotopes, the magnetic field was calibrated by measuring the cyclotron frequency of stable ^{7}Li$^+$ produced by the

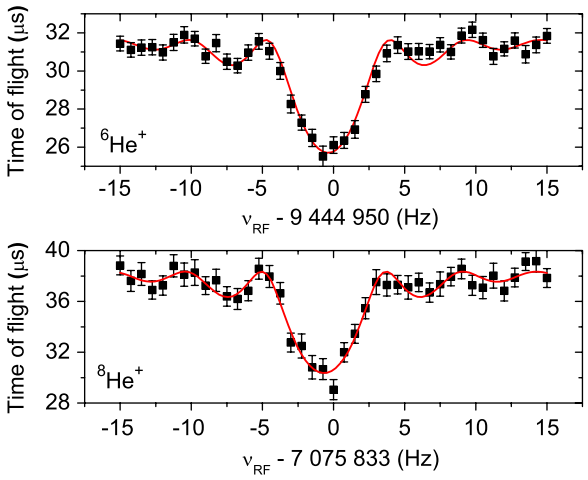

FIG. 1 (color online). Time-of-flight resonance spectra of ^{6}He$^+$ and ^{8}He$^+$. The solid line (red) is a fit of the theoretical line shape [22]. The shortest time of flight is achieved when the ions are excited at the cyclotron frequency, i.e., when $\nu_{RF} = \nu_c$.

TITAN off-line ion source between the ^{6}He$^+$ (or ^{8}He$^+$) cyclotron frequency measurements. From these measurements, one calculates the frequency ratio $R = \nu_c(^7\text{Li}^+)/\nu_c(^{6,8}\text{He}^+)$, which yields the ratio of the masses of the two ions.

A total of 12 ^{6}He$^+$ and 17 ^{8}He$^+$ frequency ratios where measured, and for these measurements, the different sources of systematic errors such as magnetic field inhomogeneities, misalignment with the magnetic field, harmonic distortion of the trap potential, nonharmonic terms in the trapping potential, interaction of multiple ions in the trap, magnetic field fluctuations over time, and error due to relativistic effects were considered (see [25] for a detailed analysis and treatment of these effects for the ^{6,8}He measurements). The main systematic errors on the ^{6}He and ^{8}He cyclotron frequency ratios arise from the interaction of multiple ions in the trap and are found to be 8 and 13 ppb for ^{6}He$^+$ and ^{8}He$^+$, respectively. The contributions from the other effects are all below the ppb level and therefore have a negligible contribution to the final uncertainty. The weighted averages of the cyclotron frequency ratios $\bar{R}$ are 0.857 868 442 9(42){82} and 1.145 098 361(7){16} for ^{6}He and ^{8}He, respectively (where the statistical uncertainty is given in parenthesis and the total uncertainty in curly brackets).

In mass spectrometry, the quantity of interest is the atomic mass, which is given by $m = \bar{R}(m_{\text{cal}} - m_e + B_{e,\text{cal}}) + m_e - B_e$, where $B_{e,\text{cal}}$ and B_e are the last electron binding energies of the calibrant ion and of the ion of interest, m_e is the electron mass, and m_{cal} is the calibrant atomic mass.

Using the more precise mass measurement of the calibrant ^{6}Li from [26], the ^{8}He mass reported in [18] becomes 8.033 935 67(72) u. The ^{8}He measurement presented here yields a mass of 8.033 934 40(12) u, which agrees with the

previous result within 1.7σ, with a factor of 12 improvement in precision. Combining these two results, the mass and mass excess of ^{8}He become 8.033 934 44(11) u and 31 609.72(11) keV. This is within 1.7σ of the atomic mass evaluation (AME03) value [8]. On the other hand, for the ^{6}He mass and mass excess we obtain 6.018 885 883(57) and 17 592.087(54) keV, which deviate from the AME03 by 4σ while improving the precision by a factor of 14.

Following the TITAN measurements, the new ^{6}He and ^{8}He two-neutron separation energies are 975.46(23) and 2125.00(33) keV, respectively. Using the new masses we also computed the charge radii of ^{6,8}He following the procedure presented in [7]. The TITAN masses enter in the mass shift $\delta\nu^{A,4}_{\mathrm{MS}}$ evaluation obtained from atomic structure calculations [4]. These new mass shifts, together with the corresponding isotopic shifts $\delta\nu^{A,4}$ from [6,7] and updated field shifts $\delta\nu^{A,4}_{\mathrm{FS}}$ are presented in Table I. The total field shift for ^{8}He was taken as the weighted average of all transitions, and the various systematic uncertainties presented in [7] were added in quadrature yielding a field shift of $-1.020(64)$ MHz. For ^{6}He, [6,7] were treated as independent measurements. Consequently, we took the weighted average of the two final field shifts, except for the Zeeman systematic uncertainty (0.03 MHz), which was present in both measurements and added in quadrature to obtain the final error. We also applied the nuclear polarization correction [$-0.014(3)$ MHz] to the measurement [6] as done in [7]. The total field shift for ^{6}He is then $-1.430(31)$ MHz. The resulting mean-square charge radii $(r_c^2)^A$ of ^{6,8}He are computed using Eq. (1), where $(r_c)^{A'=4} = 1.681(4)$ fm [27] is the mean-square charge radius of ^{4}He, and $K_{\mathrm{FS}} = 1.008$ MHz/fm^2 [4]. The updated values for the ^{6,8}He charge radii are 2.060(8) and 1.959(16) fm, respectively. The new mass measurements lead to a decrease in the ^{6}He charge radius by 0.011 fm and an increase in ^{8}He by 0.025 fm compared to the values of [7] with the ^{4}He charge radius from [27], which significantly reduces the difference between the two isotopes.

In order to compare the experimental charge radii with theory, we need to calculate the corresponding point-proton radii r_{pp} given by [28]

$$r^2_{\mathrm{pp}} = r_c^2 - R_p^2 - (N/Z)R_n^2 - 3/(4M_p^2) - r^2_{\mathrm{so}}, \qquad (2)$$

where R_p^2 and $R_n^2 = -0.1161(22)$ fm^2 [29] are the proton and neutron mean-square charge radii, respectively, $3/(4M_p^2) = 0.033$ fm^2 is a first-order relativistic (Darwin-Foldy) correction [30], and r^2_{so} is a spin-orbit nuclear charge-density correction. The latter is estimated to be -0.08 and -0.17 fm^2 in the extreme case of pure p-wave halo neutrons [28] for ^{6}He and ^{8}He, respectively (see also [31] for an improved estimate). Realistic values should be somewhere between zero and these extremes, so we conservatively took 0.08 and 0.017 fm^2 as the corresponding error.

For R_p the Particle Data Group [29] value is 0.877(7) fm. Recently, R_p has been also precisely measured from spectroscopy of muonic hydrogen [32] leading to 0.841 84 (67) fm. Using these two values for R_p with the above-mentioned spin-orbit corrections in Eq. (2) we obtain $r_{\mathrm{pp}} = 1.938 \pm 0.023$ (1.885 ± 0.048) and 1.953 ± 0.022 (1.901 ± 0.048) fm for ^{6}He (^{8}He), respectively. The experimental range in Fig. 2 includes both cases within the errors shown for ^{6}He.

In Fig. 2, we compare the point-proton radius and the two-neutron separation energy S_{2n} of ^{6}He to *ab initio* calculations based on different NN and 3N interactions. The Green's function Monte Carlo (GFMC) results [11] are the only existing converged calculations that include 3N forces, which are constrained to reproduce the properties of light nuclei, including ^{6}He and ^{8}He. The scatter in Fig. 2 gives some measure of the numerical uncertainty in the

TABLE I. Isotopic shift values from [7] (except the last transition, which is from [6]), together with the new calculated mass shifts $\delta\nu^{A,4}_{\mathrm{MS}}$ and the new field shift $\delta\nu^{A,4}_{\mathrm{FS}}$ for ^{6,8}He using the masses measured by the TITAN Penning trap spectrometer. "Mean + nucl. pol." gives the weighted mean of the transitions presented above plus the nuclear polarization correction. Statistical error is given in parentheses and the total error in curly brackets. The errors on the ^{6,8}He mass shifts are 0.8 and 0.9 kHz, respectively. All units are in MHz.

Transition	$\delta\nu^{A,4}$	$\delta\nu^{A,4}_{\mathrm{MS}}$	$\delta\nu^{A,4}_{\mathrm{FS}}$
^{8}He $2^3S_1 \rightarrow 3^3P_1$	64 701.129(73)	64 702.0982	$-0.969(73)$
^{8}He $2^3S_1 \rightarrow 3^3P_2$	64 701.466(52)	64 702.5086	$-1.043(52)$
Mean + nucl. pol.			$-1.020(42)\{64\}$
^{6}He $2^3S_1 \rightarrow 3^3P_0$	43 194.740(37)	43 196.1573	$-1.417(37)$
^{6}He $2^3S_1 \rightarrow 3^3P_1$	43 194.483(12)	43 195.8966	$-1.414(12)$
^{6}He $2^3S_1 \rightarrow 3^3P_2$	43 194.751(10)	43 196.1706	$-1.420(10)$
Mean + nucl. pol.			$-1.431(8)\{31\}$
^{6}He $2^3S_1 \rightarrow 3^3P_2$	43 194.772(33)	43 196.1706	$-1.399(33)\{50\}$
Mean			$-1.430(8)\{31\}$

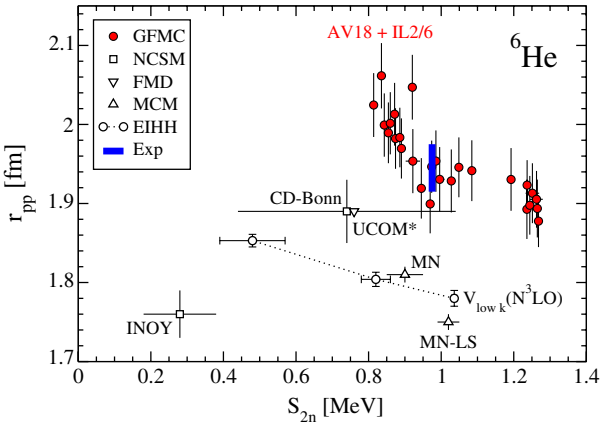

FIG. 2 (color online). Correlation plot of the ^{6}He point-proton radius r_{pp} versus two-neutron separation energy S_{2n}. The experimental range (bar) is compared to theory based on different *ab initio* methods using different NN interactions only (open symbols) and including $3N$ forces fit to light nuclei (filled symbols). The *ab initio* methods are indicated in the legend and the nuclear forces next to the symbols (for details see text). Theoretical error bars are shown where available.

GFMC method as well as an uncertainty in the $3N$ force models used [the Illinois 2 and 6 (IL2 and IL6) three-body forces were used with the Argonne v18 (AV18) NN potential] [11]. The comparison of the experimental range to theory clearly demonstrates the importance of including and advancing $3N$ forces. The theoretical results shown in Fig. 2 based on NN interactions only are consistently at lower S_{2n} and smaller r_{pp} values. The NN-only calculations include the fermionic molecular dynamics (FMD) results based on the unitary correlation operator method (UCOM) NN potential and a phenomenological term (to account for three-body physics) [13], the no-core shell model (NCSM) results based on the charge-dependent (CD) Bonn and inside nonlocal outside Yukawa tail (INOY) NN potentials [12], and variational microscopic cluster model (MCM) results based on the Minnesota (MN) and MN without spin-orbit (MN-LS) NN potentials [14]. Figure 2 also shows the importance of comparing theoretical predictions to more than one observable. To illustrate this, both NCSM (using CD Bonn) and the GFMC results show a good agreement for the point-proton radius, while the NCSM result has a large error for S_{2n} and tends to underpredict the two-neutron separation energy.

In addition, we present new effective interaction hyperspherical harmonics (EIHH) results [15] based on chiral low-momentum NN interactions $V_{\text{low } k}$ [33]. In the EIHH approach the wave function falls off exponentially by construction, making it ideally suited for the study of halo nuclei (for calculational details see [15]). The obtained energies and radii are converged within the few-body calculational uncertainty given by the error bars. The three EIHH results shown in Fig. 2 are for different NN cutoff scales $\Lambda = 1.8$, 2.0, and 2.4 fm^{-1}. The running of observables with Λ is due to neglected many-body forces. The EIHH results lie on a line indicated in Fig. 2, leading to a decreasing S_{2n} and increasing r_{pp}, that does not go through the experimental range. Such a correlation is expected, because a smaller S_{2n} stretches out the core [7]. This correlation is also similar to the Phillips and Tjon lines in few-body systems [34], which arise from strong NN interactions (large scattering lengths). Three-body physics manifests itself as a breaking from this line or band. The correlation is also supported by the variational MCM results. A key future step will be to include chiral $3N$ forces in the EIHH calculations.

We have presented the first direct mass measurement of the two-neutron halo nucleus ^{6}He and a more precise mass value for the four-neutron halo ^{8}He. Both measurements where performed using the TITAN Penning trap mass spectrometer. While the ^{8}He mass value is 1.7σ within the AME03 [8], the ^{6}He mass deviates by 4σ. The new masses lead to improved values of the charge (and point-proton) radii and the two-neutron separation energies, which combined provide stringent tests for three-body forces at neutron-rich extremes.

This work was supported by the Natural Sciences and Engineering Research Council of Canada (NSERC) and the National Research Council of Canada (NRC). We would like to thank the TRIUMF technical staff, especially Melvin Good. S. E. acknowledges support from the Vanier CGS program, T. B. from the Evangelisches Studienwerk e.V. Villigst, D. L. from TRIUMF during his sabbatical, and A. S. from the Helmholtz Alliance HA216/EMMI.

*Corresponding author.
brodeur@nscl.msu.edu
†Present address: National Superconducting Cyclotron Laboratory, Michigan State University, East Lansing, MI 48824, USA.

[1] I. Tanihata, J. Phys. G **22**, 157 (1996).
[2] B. Jonson, Phys. Rep. **389**, 1 (2004).
[3] P. G. Hansen and B. Jonson, Europhys. Lett. **4**, 409 (1987).
[4] G. W. F. Drake, Nucl. Phys. **A737**, 25 (2004).
[5] W. Nörtershaüser *et al.*, Phys. Rev. A **83**, 012516 (2011).
[6] L. B. Wang *et al.*, Phys. Rev. Lett. **93**, 142501 (2004).
[7] P. Mueller *et al.*, Phys. Rev. Lett. **99**, 252501 (2007).
[8] G. Audi, A. H. Wapstra, and C. Thibault, Nucl. Phys. **A729**, 337 (2003).
[9] R. G. H. Robertson *et al.*, Phys. Rev. C **17**, 4 (1978).
[10] M. Smith *et al.*, Phys. Rev. Lett. **101**, 202501 (2008).
[11] S. C. Pierper, Riv. Nuovo Cimento **31**, 709 (2008).
[12] E. Caurier and P. Navratil, Phys. Rev. C **73**, 021302 (2006).
[13] T. Neff, H. Feldmeier, and R. Roth, Nucl. Phys. **A752**, 321c (2005).
[14] I. Brida and F. M. Nunes, Nucl. Phys. **A847**, 1 (2010).
[15] S. Bacca *et al.*, Eur. Phys. J. A **42**, 553 (2009); (to be published).

[16] J. Dilling *et al.*, Int. J. Mass Spectrom. **251**, 198 (2006).
[17] M. Dombsky *et al.*, Rev. Sci. Instrum. **71**, 978 (2000).
[18] V. Ryjkov *et al.*, Phys. Rev. Lett. **101**, 012501 (2008).
[19] P. Bricault *et al.*, Rev. Sci. Instrum. **79**, 02A908 (2008).
[20] M. Smith *et al.*, Hyperfine Interact. **173**, 171 (2006).
[21] G. Gräff, H. Kalinowsky, and J. Traut, Z. Phys. A **297**, 35 (1980).
[22] M. König *et al.*, Int. J. Mass Spectrom. Ion Process. **142**, 95 (1995).
[23] M. Brodeur *et al.*, Phys. Rev. C **80**, 044318 (2009).
[24] M. Brodeur *et al.*, Int. J. Mass Spectrom. **310**, 20 (2012).
[25] M. Brodeur, Ph.D. thesis, University of British Columbia, 2010.
[26] B. J. Mount, M. Redshaw, and E. G. Myers, Phys. Rev. A **82**, 042513 (2010).
[27] I. Sick, Phys. Rev. C **77**, 041302(R) (2008).
[28] A. Ong, J. C. Berengut, and V. V. Flambaum, Phys. Rev. C **82**, 014320 (2010).
[29] K. Nakamura *et al.* (Particle Data Group), J. Phys. G **37**, 075021 (2010).
[30] J. L. Friar, J. Martorell, and D. W. L. Sprung, Phys. Rev. A **56**, 4579 (1997).
[31] G. Papadimitriou *et al.*, Phys. Rev. C **84**, 051304(R) (2011).
[32] R. Pohl *et al.*, Nature (London) **466**, 213 (2010).
[33] S. K. Bogner, R. J. Furnstahl, and A. Schwenk, Prog. Part. Nucl. Phys. **65**, 94 (2010).
[34] P. F. Bedaque and U. van Kolck, Annu. Rev. Nucl. Part. Sci. **52**, 339 (2002).